Remanent flux creep in $YBa_2Cu_3O_{7-\delta}$ films in the critical region

I. P. Krylov
Department of Physics, University of the Western Cape, Bellville 7535, South Africa

E. J. Maritz and E. B. Nyeanchi
Van de Graaff Group, National Accelerator Centre, Faure 7131, South Africa

(Received 3 April 1997; revised manuscript received 13 May 1998)

The remanent magnetic flux creep in $YBa_2Cu_3O_{7-\delta}$ thin films was investigated in the vicinity of the critical temperature T_c. The trapped magnetic flux was generated in the specimen by ramping the applied field to a finite value and then back to zero. The remanent magnetic field of persistent currents circulating in the sample was measured as a function of temperature and time. Data on the critical current density j_c and the creep activation energy U were extracted. A sharp decrease of U at temperatures $T_c - T \lesssim 1$ K was related to critical fluctuations. In this critical region a power-law time decay of the currents $j \propto t^{-p}$ was observed and explained by the logarithmic dependence $U = U_0 \ln(j_c/j)$ for the current-assisted thermal unbinding of vortex-antivortex pairs generated by the critical fluctuations. In the critical region, the temperature dependence $j_c \propto (T_c - T)^2$ was observed. A possibility to relate this result to the critical behavior of the three-dimensional XY model is discussed. [S0163-1829(98)07545-6]

I. INTRODUCTION

Studies of magnetic flux vortices occupy an outstanding place in the history of high-temperature superconductors (HTSC's). The tremendous theoretical effort was summarized in the monumental review by Blatter *et al.*[1] Thermally activated motion of vortices, so called flux creep became, in its own right, an important part of HTSC research. Experimental studies of flux creep were reviewed in a recent paper by Yeshurun *et al.*[2] Most of the work was done in the region of the magnetic field—temperature B-T phase space, which lies outside the regime of critical fluctuations. The latter is determined by the Ginsburg number

$$Gi = \frac{1}{2}\left(\frac{kT_c}{H_c^2(0)\varepsilon\xi^3(0)}\right)^2 = 32\pi^4\left(\frac{kT_c\lambda(0)\kappa}{\Phi_0^2\varepsilon}\right)^2,$$

with the usual notation of the Boltzmann constant k, critical temperature T_c, thermodynamic critical field $H_c(T)$, Ginsburg-Landau (GL) coherence length $\xi(T)$, and flux quantum Φ_0. In $YBa_2Cu_3O_{7-\delta}$ (YBCO) with the known values of GL penetration depth $\lambda(0) \simeq 10^{-5}$ cm, GL parameter $\kappa = \lambda/\xi \simeq 100$, and anisotropy ratio $\varepsilon = \sqrt{m/M} \simeq 1/7$, the number acquires the value $Gi \simeq 1.5 \times 10^{-2}$. In the temperature interval $|T_c - T| < Gi \times T_c \simeq 1$ K, which is referred to as the critical region, the fluctuations in the amplitude of the order parameter $|\psi|$ are of the same order as $|\psi|$ itself. Outside this region all the fluctuation degrees of freedom involve only the phase of the order parameter, which can be described by fluctuations in the positions of the vortices.[1] It is in this part of the phase diagram where an impressive number of theoretical results has been obtained and successfully applied to explain the abundant experimental data.

By contrast, the critical region is at present a matter of debate with limited experimental results available. The main question is the universality class of the transition. In support of the initial idea of Lobb,[3] there is growing evidence that YBCO exhibits critical behavior of the three-dimensional (3D) XY model, in which case its superconducting transition belongs to the same universality class as the superfluid transition in liquid ^{4}He. Measurements of the specific heat[4,5] and microwave penetration depth in zero field[6,7] were consistent with the critical behavior of the 3D XY model. In Refs. 5,6 the experimental data were fitted to theory over the temperature range $\Delta T \simeq 10$ K near T_c.

This value is evidently too large when compared with the width of the superconducting transition in zero field $\Delta T < 1$ K. In fact, the early data[8] on paraconductivity above T_c suggested that the width of the critical region was $\simeq 0.5$ K, in agreement with the Lobb prediction.[3] However, it was argued[9] that the point where the system crosses over from mean-field to fluctuation-dominated behavior could be lower than expected from the traditional Ginsburg criterion, giving the critical region width of the order of 10 K. It is thus important to probe the critical region with a different experimental method.

In this paper we report measurements of the remanent flux creep done over a range of temperatures up to $T_c - T \leqslant 0.05$ K, where it was experimentally possible to get into the usually inaccessible long-time limit of persistent current relaxation. In the previous measurements of flux creep near T_c,[10–12] the range $T_c - T < 1$ K was not resolved. The present results show that a sharp decrease in the creep activation energy U occurs in the range $\Delta T \lesssim 1$ K, suggesting that the critical region is being entered. A power-law time decay of the persistent currents in the critical region $j \propto t^{-p}$ indicates that the creep activation energy is a logarithmic function of the current density $U = U_0 \ln(j_c/j)$, which can be explained easily, if the critical fluctuations are assumed to generate vortex-antivortex pairs interacting via the familiar logarithmic potential and dissociating in the presence of the current. But under this assumption, the mean-field energy scale in the vortex pair potential has to be modified to fit the 3D XY critical behavior to the observed temperature depen-

dence $j_c \propto (T_c - T)^2$. The exponent in this power law is determined experimentally with precision $\sim 2\%$. This is the main result of the present work.

II. EXPERIMENT

A. Samples

The YBCO films used in our experiments were prepared by sputtering or by pulsed laser deposition on MgO, $LaAlO_3$, or $SrTiO_3$ substrates of size 10×10 mm^2. The superconducting transition temperature determined by dc resistivity or ac susceptibility methods was in the range 87–89 K with the width of transition about 1 K or less. The films were of good epitaxial quality with the c axis normal to the film plane. All the films showed similar behavior. The particular data presented below in Figs. 1–3 were obtained with the film of thickness $d = 3 \times 10^{-5}$ cm on $LaAlO_3$ supplied by ''Conductus.'' The resistive measurements with this sample showed the narrowest superconducting transition of half-width $\Delta T_{1/2} \simeq 0.2$ K and temperature $T_{cR} \simeq 89.0$ K (at $T \leqslant T_{cR}$ the resistance was below the sensitivity limit $R \simeq 10^{-4} R_n$, at $T = T_{cR} + \Delta T_{1/2}$ the resistance was half of the value R_n extrapolated from the linear part well above the transition).

B. Temperature control

During the experiments the temperature of the sample was controlled and stabilized in the range $77.5 \text{ K} < T < 95$ K. For that purpose the sample was placed inside a cylindrical copper block of thickness 3 mm and diameter 16 mm with a recess for the sample in the middle of the block. The film substrate was clamped to the copper surface, with a layer of vacuum grease in between to improve the thermal contact. A heater and a silicon diode temperature sensor were glued to the outer flat surface of the copper cylinder with a thermally conductive varnish. The copper block was covered with a polystyrene thermal insulator, and this sample holder was immersed in liquid nitrogen. When the heater was off, the liquid filled the sample holder, but as soon as the heater power was $\geqslant 0.02$ W, the nitrogen inside the block evaporated. The usual heater power to provide the desired temperatures was ~ 0.1 W, and the nitrogen vapor at atmospheric pressure served as a heat exchange gas inside the block. The geometry of the system and the standard data for the copper thermal conductivity 5 W/cm K permitted us to estimate the possible temperature gradients inside the block $\delta T_{b1} \lesssim 5$ mK. The noise limited sensitivity of the temperature sensor was about 2 mK. The short term ($t < 10$ min) stability during the flux decay runs was of the same order of magnitude. The temperature instability during long runs, which took up to 3 h, was < 20 mK.

In special tests our temperature sensor was compared with a calibrated silicon diode of absolute accuracy ± 50 mK, which determined the absolute accuracy of all reported temperature values in the range 77–90 K. Note that the important results were related to small changes of temperature, which were measured with the accuracy of several millikelvin, and the absolute accuracy of the critical temperature did not matter.

C. Magnetic field measurement

We used a HTSC superconducting quantum interference device (SQUID) magnetometer of noise limited sensitivity $\sim 10^{-6}$ G to measure the magnetic field of the currents circulating in the sample. The sample holder with a small surrounding solenoid was positioned near the SQUID sensor (SQUID input coil) inside a liquid nitrogen cryostat, the typical distance between the sample and the sensor being ~ 1 cm. The cryostat was inside a three-layer mu-metal magnetic shield of shielding efficiency above 100 dB. Thus the stray field of the order of 10^{-6} G was negligible when compared with the field created in the film by the circulating currents. The same was true for the field produced by the SQUID at the surface of the sample, because the operating field of the SQUID feedback coil $< 10^{-2}$ G was decreased 10^5 times due to the very small size of the feedback coil (≈ 0.1 mm) when compared with the distance to the sample.

After zero-field cooling and stabilizing the sample temperature below T_c, the current through the small solenoid was switched on. The external magnetic field perpendicular to the film surface was increased up to a value B_0, high enough to produce a critical state in most of the film, where screening superconducting currents had a critical density j_c. The external field was then reduced to zero. A remanent flux parallel to the magnetizing field was trapped inside the film due to the pinning of vortices. Accordingly, the superconducting currents of critical density continued to circulate in the film in the direction opposite to the initial screening currents. The required characteristic value of the magnetizing field B_0 was ~ 3 G at $(T_c - T) \sim 1$ K, and increased proportionally to j_c up to 100 G at $(T_c - T) \simeq 10$ K. The magnetizing cycle took $\simeq 20$ s. The results reported here were independent of the exact values of B_0 or the ramp rate.

D. Interpretation of the SQUID signal

To interpret the SQUID signal in terms of currents circulating in the sample, we approximated our square films by a disc of radius $R = 0.5$ cm, and introduced cylindrical coordinates (r, φ, z) with the z axis perpendicular to the film, and $r = z = 0$ in the center of the sample. Due to assumed axial symmetry, there was only a circumferential nonzero component of the current density vector $j_\varphi = j$. The magnetic field sensor was positioned on the z axis at a distance $z > R$ to measure the component B_z. In thin films the currents can be treated as uniform in the z direction (see, e.g., Ref. 13). The value B_z can then be related to the currents by the formula

$$B_z = \frac{2\pi d}{c} \int_0^R \frac{j r^2 dr}{(r^2 + z^2)^{3/2}}. \tag{1}$$

The critical current density was assumed to be independent of the local density of trapped vortices. Thus in the remanent critical state we used the results of the theoretical treatment[14] which gave the density $j = j_c = \text{const}$ for $b \leqslant r \leqslant R$, where the penetration radius

$$b = \frac{R}{\cosh(c B_0 / 4\pi j_c d)}.$$

The contribution to the integral in Eq. (1) from the central part of the film at $r \ll R < z$ is small. Usually the penetration radius was $b \sim 1$ mm, and the contribution of the region $r \leqslant b$ was $\sim 1\%$. We therefore assumed $j = \text{const}$ and calculated the integral in Eq. (1) to obtain the formula

$$B_z = \frac{2\pi j d}{c}\left[\ln\left(\frac{R+\sqrt{R^2+z^2}}{z}\right) - \frac{R}{\sqrt{R^2+z^2}}\right].$$

It was used to calculate the current density j from the SQUID signal $F \equiv B_z$ at the known geometrical parameters d, R, z. Due to the approximations made, the data presented below give only the order of magnitude of the critical current density. But since the relative position of the SQUID sensor and the sample was fixed, the accuracy of time and temperature dependences in which we are interested, were not compromised.

E. Experimental procedure

After the magnetizing cycle, we distinguished two types of experimental runs: an isothermal flux decay and a warm up. During the flux decay run, the isothermal relaxation of the SQUID signal $F(t)$ was recorded for time intervals from several minutes up to 3 h. The remanent flux decay occurred due to flux creep, and was equivalent to the decrease of circulating superconducting currents, and consequently the measured field B_z. In these runs the data on the flux creep activation energy $U = U(j,T)$ were obtained as discussed below. Typical experimental curves are presented in Fig. 1. The magnetic signal followed a power-law time decay

$$\frac{F}{F_0} = \frac{1}{(1+t/t_0)^p}$$

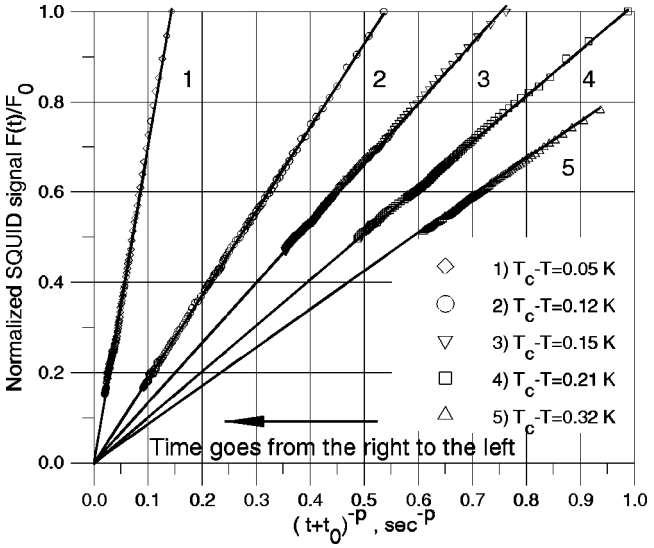

FIG. 1. Remanent flux relaxation at various temperatures in the vicinity of $T_c = 88.77$ K. Experimental points represent the SQUID signal $F(t) \propto (t+t_0)^{-p}$. The fitting parameters for the different curves are (1) $p = 0.78$, $t_0 = 12$ s, (2) $p = 0.34$, $t_0 = 4$ s, (3) $p = 0.18$, $t_0 = 0.3$ s, (4) $p = 0.12$, $t_0 = 0$ s, (5) $p = 0.087$, $t_0 = 0$ s. The normalization factor is $F_0 = F(t = 1.1$ s), except (3) $F_0 = F(t = 4$ s) and (5) $F_0 = 1.3F(t = 2$ s). The solid straight lines are the results of linear regression analysis of experimental data.

with a parameter $p < 1$ and a time scale t_0, which could be experimentally determined as nonzero only very close to T_c. This type of decay has been reported before in several experiments.[1,2] For not very long relaxation such that $\ln(t/t_0) \ll 1/p$, the power-law dependence could be approximated by the well known logarithmic decay

$$F/F_0 \simeq 1 - p\ln(1+t/t_0).$$

This occurred well below T_c where $p \leqslant 0.05$ for the whole duration of the decay run. The temperature dependence of the fitting parameter p is presented in Fig. 2 as the data on the initial flux creep activation energy $U_0/kT = 1/p$ in agreement with theory discussed below. The large scatter of the experimental points is due to a temperature instability during the long decay runs.

The data on temperature dependence of the critical current density $j_c = j_c(T)$ was obtained conveniently during the warming runs. After the magnetization and short relaxation at some temperature $T_1 < T_c$, the heater power was increased, and for several minutes the sample was warmed above the critical temperature. Throughout the warm up, the magnetometer continuously monitored the magnetic field of superconducting currents $j_1(T)$ circulating in the film. The warming rate of ~ 10 mK/s was fast enough to register nonrelaxed density $j_1(T) \simeq j_c(T)$, as discussed in detail below. The SQUID started to monitor the nonrelaxed currents when the value $j_1(T)$ was well below the relaxed value at the starting temperature T_1. Typical experimental curves obtained in the warming runs are presented in Figs. 2 and 3.

F. Temperature of the sample

To verify that the warming rate was adequate to give $j_1(T) \simeq j_c(T)$, and at the same time to check a possible temperature difference between the sample and the copper block, warming runs were done at various temperature rates $\dot{T}_b$ of the measured copper block temperature T_b. The starting temperature T_1 was about 1 K below T_c. The time constant of the magnetometer and the rest of the data acquisition system was ~ 0.2 s. The experiments showed that the $j_1(T_b)$ dependence shifted as a whole to higher temperatures with the shift $\delta T_b \propto \dot{T}_b$ in the range 10 mK/s $\leqslant \dot{T} \leqslant 40$ mK/s, being $\simeq 90$ mK at $\dot{T}_b = 40$ mK/s.

The analysis of the thermal conductivity equation shows that at $\dot{T}_b = \text{const}$ the sample temperature follows the block temperature with the same time derivative but shifted by the characteristic time τ_1 which is determined by the sample heat capacity and the thermal resistance between the film and the surrounding copper block. The abovementioned data on the experimentally observed shift $\delta T_b = \dot{T}_b \tau_1$ gave us the value $\tau_1 = 2.2$ s with an accuracy $\simeq 10\%$. The sample temperature could thus be determined during the warming runs of $\dot{T}_b < 10$ mK/s with precision limited only by the accuracy of the T_b measurements, i.e., 2 mK. In fast runs of $\dot{T}_b \geqslant 10$ mK/s, the error in determination of the sample temperature was proportionally higher.

For any change of the block heating regime the sample relaxed to the new regime with the same relaxation time τ_1. Evidently, at $T_b = \text{const}$ the sample temperature was T

$=T_b$. The dynamic temperature gradients inside the copper block could be estimated to be at least 10 times smaller than the possible static gradients $\delta T_{b1} \lesssim 5$ mK.

G. Creep freezing effect

An additional experimental check of the sample temperature control was done during the experiments on the creep freezing effect. Although this effect was reported earlier in experiments at low temperatures (see references in Ref. 2), we would like to discuss briefly how it occurred in the critical region. An experimental run was as follows. The magnetizing cycle was made at the sample temperature $T=T_1$. At some moment of isothermal relaxation the heating power was decreased and the sample cooled. During this process the film temperature T could be determined with a sufficient accuracy from the measured block temperature T_b as discussed above.

The flux creep relaxation rate responded sharply to the decrease of temperature. Within the interval $\delta T_f = T_1 - T = 10$ mK the flux relaxation rate $|dF/dt|$ dropped several times, and at still lower temperatures became practically zero. At $(T_1 - T) > 0.2$ K in the range of $0.3\ \text{K} \leqslant (T_c - T_1) \leqslant 1$ K, the magnetic flux was completely frozen inside the sample, and the SQUID showed a constant field for hours. After the freezing stage the temperature of the sample was raised, usually at the same rate $|\dot{T}_b| = \text{const}$ as during cooling (1–10 mK/s). The SQUID signal remained stationary within the sensitivity limit (0.1%) until the rising temperature reached the value $T \simeq T_1 - 10$ mK. Then within an interval $\simeq 10$ mK the flux creep recovered its initial value $|dF/dt|_1$ which occurred before freezing, and as the temperature continued to grow linearly with time, the signal dropped exponentially for several seconds more, finally approaching much lower values corresponding to the lower j_c at elevated temperatures $T > T_1$.

The creep freezing effect can be explained easily. For algebraic simplicity the logarithmic time decay relation $j/j_c = 1 - p \ln(t/t_0)$ at $t \gg t_0$ and $p \ll 1$ is used. Then the creep rate is

$$\frac{1}{j_c}\frac{dj}{dt} = -\frac{p}{t} = -\frac{p}{t_0}\exp\left(-\frac{j_c - j}{p j_c}\right).$$

Suppose at some moment the temperature starts to decrease fast, and the currents in the sample j stay approximately constant, but the value j_c grows. Then one can write for a small increase $\delta j = j_c(T) - j_c(T_1) \ll j_c(T_1) \equiv j_{c1}$ the relation $dj/dt = (dj/dt)_1 \exp(-\delta j/p j_{c1})$, where $(dj/dt)_1$ is the decay rate just before freezing started. For $j_c \propto (T_c - T)^2$ and $\delta T = T_1 - T$, one has $\delta j/j_{c1} = 2\,\delta T/(T_c - T_1)$ and

$$\frac{dj}{dt} = \left(\frac{dj}{dt}\right)_1 \exp\left(-\frac{2\,\delta T}{p(T_c - T_1)}\right).$$

It is clear that a relatively small decrease in temperature $\delta T > 0$ can result in a great drop of the relaxation rate, because $p \ll 1$. For $(T_c - T_1) = 1$ K the value $p \simeq 0.02$, and the characteristic temperature interval becomes $\delta T_f = p(T_c - T_1)/2 = 10$ mK, in good agreement with the experimental observations. The relation for dj/dt can be integrated easily for the whole freezing-unfreezing cycle in the case of temperature sweeps which are linear in time. The result shows that the flux starts to unfreeze when the temperature approaches T_1, and the value

$$j = j_{\text{fr}} + \left(\frac{dj}{dt}\right)_1 \frac{\delta T_f}{|\dot{T}_b|}\exp\left(\frac{T - T_1}{\delta T_f}\right),$$

where j_{fr} corresponds to the frozen flux signal at $T \ll T_1$.

This discussion of the freezing-unfreezing effect confirms that the sample temperature was well controlled with an accuracy < 10 mK. Note that the inhomogeneity of the sample which could cause the critical current inhomogeneity is not detrimental to the sharp freezing-unfreezing effect because at each point of the sample the initial difference $(j_c - j)/j_c$ at the freezing start is the same, although j_c and j can vary across the sample.

III. ANALYSIS OF RESULTS

A. Nonlinear diffusion equation

The trapped flux relaxation is determined by the nonlinear diffusion equation (NDE) for currents and fields.[1,13] For a plate in a parallel magnetic field, the NDE has been solved[15] exactly in the case of a logarithmic barrier $U = U_0 \ln(j_c/j)$ with $\sigma \equiv U_0/kT \gg 1$. The solution yields a power-law time decay $j/j_c \simeq (1 + t/t_0)^{-1/\sigma}$ with a macroscopic time scale t_0. As can be seen in Fig. 1, that is the type of decay observed experimentally with the fitting parameter $p = 1/\sigma$. To verify the validity of the solution and to calculate the time constant t_0 in our case, we have to derive and solve the NDE for a film magnetized in a perpendicular field. We suppose that a solution of this problem for a thin disc can give us a qualitatively correct description of the observed phenomena.

The NDE is determined by the Maxwell equations and the nonlinear relation between the current density and the electrical field $E = E(j)$. The axial symmetry provides the only nonzero circumferential components of both **E** and **j** vectors, which are uniform in the z direction in thin films. Therefore, the Maxwell equations give

$$\frac{4\pi}{c^2}\frac{\partial j}{\partial t} = \frac{\partial}{\partial r}\left(\frac{1}{r}\frac{\partial (rE)}{\partial r}\right).$$

To construct the nonlinear relation $E = E(j)$, we follow the line of ideas proposed in Ref. 15. The vortex drift velocity $v = v_0 e^{-U/kT}$ is introduced for a thermally activated motion of vortices with a characteristic velocity $v_0 \sim c j_c \rho_n / H_{c2} \sim 10^3$ cm/s for a free vortex flow without pinning.[1] The logarithmic barrier relation $U = U_0 \ln(j_c/j)$, which also defines the theoretical parameter j_c, gives $v = v_0 (j/j_c)^{\sigma}$. Following Ref. 1 the electrical field is assumed to be proportional to the vortex drift velocity. This leads to the relation

$$E = \frac{4\pi}{c^2} v_0 d \left(\frac{j}{j_c}\right)^{\sigma} j,$$

where an additional factor $\propto j$ appears because the magnetic field in the film is generated by the current itself. This relation forms the basis of the present model to derive the NDE

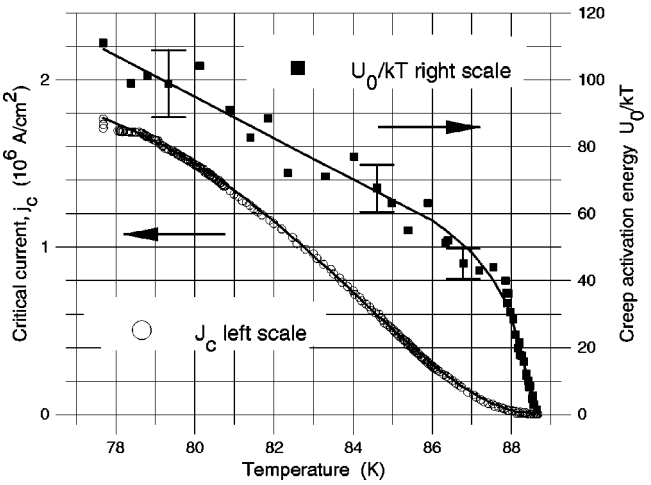

FIG. 2. Temperature dependence of the critical current density j_c and the relative creep activation energy U_0/kT, determined as described in the text. The experimental error for j_c data is less than the symbol size. The solid lines are guides to the eye.

$$\frac{\partial j}{\partial t}=v_0 d\frac{\partial}{\partial r}\left(\frac{1}{r}\frac{\partial(rj^{\sigma+1}/j_c^{\sigma})}{\partial r}\right). \tag{2}$$

Away from the disc center, an approximate solution of Eq. (2) can be found by separation of variables $j=j_1(t)g(r)$ in the case of constant $\sigma\gg 1$ and uniform $j_c=\text{const}$. The solution of the lowest decay rate is

$$j=j_c\left[\frac{(r/R)(2-r/R)}{1+\sigma t/t_0'}\right]^{1/\sigma}, \tag{3}$$

where the time scale constant $t_0'=R^2/(3v_0 d)\sim 3$ s. A fast relaxation from the initial state after the magnetizing cycle $j(t=0)=j_c$ to the profile $j/j_c=g(r)=[(r/R)(2-r/R)]^{1/\sigma}\leqslant 1$ at $b\leqslant r\leqslant R$, occurs during the interval $t\lesssim t_0'/\sigma$. After that Eq. (3) is valid, and the space profile remains unchanged. It should be noted that for $\sigma\gg 1$ the space part function $g\simeq 1$ except very close to $r=0$, e.g., at $r=b\sim 0.2R$ and $\sigma=50$, one has $g=0.97$.

The time dependence $j_1\propto t^{-1/\sigma}$ at $t\gg t_0'$ agrees well with experiment. The important parameter $\sigma=U_0/kT=1/p$ is determined by fitting. The experimental data in this part are presented in Fig. 2. Although the formula for $j_1(t)$ is obtained under the condition $\sigma\gg 1$, further analysis shows that in the peripheral part of the disc at $0.5\leqslant r/R\leqslant 1$ it is approximately valid down to $\sigma\sim 1$. This periphery is actually the part of the sample which gives the main contribution ($\approx 90\%$) to the SQUID signal. Therefore the power-law time decay is observed down to low values of $\sigma=1/p$ as shown in Fig. 1.

A small time constant $t_0=t_0'/\sigma$, could not be resolved experimentally except very close to T_c. The theoretical estimates of t_0 are in fairly good agreement with experiment, taking into account a very crude estimate of t_0', where the possible temperature dependence of v_0 is neglected. Moreover, sample inhomogeneity only allows an order of magnitude comparison, as will be briefly discussed later.

B. Critical current

The differential equation for the time dependent part $j_1(t)$ follows from Eq. (2):

$$\frac{dj_1}{dt}=-\frac{j_1}{t_0'}\left(\frac{j_1}{j_c}\right)^{\sigma}. \tag{4}$$

It leads to a relation between the variable $j_1=j_1(t)$ which is measured during the warming runs, and the theoretical parameter $j_c=j_c(t)$. For the constant warming rate $\dot{T}$ the dependence $j_1\propto(\tau_2-t)^2$ is observed over a range of ~ 1 K near T_c. The duration of the run is $\tau_2=(T_c-T_1)/\dot{T}$, where the starting temperature $T_1<T_c$. To satisfy Eq. (4), one has to put

$$j_c=j_1\left(\frac{\tau_2-t}{2t_0'}\right)^{1/\sigma}=j_1\left[\frac{T_c-T(t)}{2t_0'\dot{T}}\right]^{1/\sigma}, \tag{5}$$

where σ is also a function of temperature and consequently time during the warm up. When the temperature is not very close to T_c and $\sigma\gg 1$ it leads to

$$j_1\simeq j_c\left[1-\frac{1}{\sigma}\ln\left(\frac{T_c-T}{2t_0'\dot{T}}\right)\right]. \tag{6}$$

Due to high values of σ at $(T_c-T)\sim 1$ K, we have $j_1\simeq j_c$ with an accuracy $\sim 5\%$ or better for fast warming ($\dot{T}\geqslant 10$ mK/s). As the temperature goes up $T\to T_c$, and the logarithm in Eq. (6) decreases, so does the denominator σ. Actual data on σ were used with Eq. (5) to calculate the ratio j_1/j_c. These calculations showed that the measured value was $j_1\simeq j_c$ accurate to $\sim 5\%$ down to $T_c-T\simeq 0.2$ K. Closer to T_c the analysis became complicated, and it was left for future investigations.

The fast warming runs proved experimentally that $j_1\simeq j_c$, because the observed dependence $j_1(T)$ did not vary with the warming rate if we took into account the shift between the measured temperature of the copper block T_b and the sample temperature T. During a slow warm up with the rate $\dot{T}\lesssim 1$ mK/s, the measured values $j_1(T)$ were lower than for the fast runs, especially near the critical temperature where j_1 turned down to zero at $T<T_c$.

C. Sample inhomogeneity

To analyze the influence of sample inhomogeneity on the warming run data, we suppose that it causes local changes of critical temperature, but the functional dependence $j_c=j_c(T_c-T)$ remains the same. It is assumed that the maximum critical temperature is T_c, and the values of critical temperature at different points of the sample are in an interval ΔT below T_c. The inhomogeneity is characterized by a distribution function $f(x)$ such that the contribution to the SQUID signal from the parts of critical temperature $T_c'=T_c-x\Delta T$ is $\propto f(x)dx$ with $0\leqslant x\leqslant 1$ and the normalization condition $\int_0^1 f(x)dx=1$. Actually, $f(x)$ is proportional to an integral of the factor $r/(r^2+z^2)^{3/2}$ over the film volume with the critical temperature T_c', as follows from Eq. (1).

For all reasonable functions $j_c(T_c-T)$, the relative influence of the inhomogeneity decreases at $(T_c-T)\gg\Delta T$. Fig-

ure 3 suggests that $j_c \propto (T_c' - T)^2$. Therefore, the SQUID signal at the temperature $T \leqslant T_c - \Delta T$ is proportional to

$$F(T) = \int_0^1 f(x)(T_c - x\Delta T - T)^2 dx = (T_c^* - T)^2 + (\Delta T^*)^2,$$

where the new parameters are

$$T_c^* = T_c - I_1 \Delta T \quad \text{and} \quad \Delta T^* = \sqrt{I_2 - I_1^2}\,\Delta T,$$

with the distribution moments

$$I_1 = \int_0^1 x f(x) dx \quad \text{and} \quad I_2 = \int_0^1 x^2 f(x) dx.$$

The functional dependence $F(T)$ below $(T_c - \Delta T)$ is determined by two parameters only, T_c^* and ΔT^*, and at $(T_c^* - T) \gg \Delta T^*$ one obtains a straight line $\sqrt{F} \simeq (T_c^* - T)$. Extrapolating this straight line to $F = 0$, one obtains the parameter T_c^*, as shown in Fig. 3.

Closer to T_c where $T > T_c - \Delta T$, the upper limit in the integrals I_1 and I_2 is a function of T. Instead of unity, the upper limit is $x_m = (T_c - T)/\Delta T < 1$, and the function $F(T)$ reveals more information about the distribution function $f(x)$. Figure 3 suggests that there is a sharp peak of $f(x)$ at $x = 0$ of integral intensity $A = \int_0^{x_1} f(x) dx$, where $x_1 \ll x_m$. Therefore as $T \to T_c$, the flux is proportional to $F = A(T_c - T)^2$. The data presented in Fig. 3 were fitted to the inhomogeneity hypothesis with the parameters $A = 0.30$, $I_1 = 0.59$, $I_2 = 0.55$, $\Delta T = 0.134$ K. This fitting set corresponds to the 30% sharp peak at T_c, and the rest spread as a broad peak of width $\simeq 0.06$ K positioned near $T_c' = T_c - 0.10$ K.

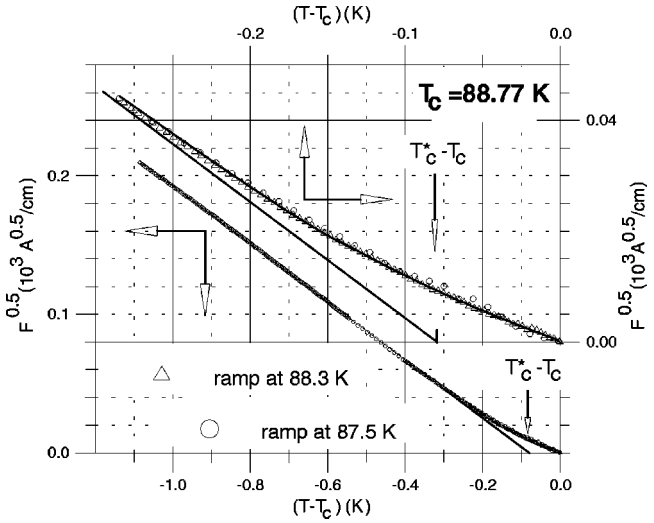

FIG. 3. Temperature dependences of $\sqrt{F}$ in the critical region. The SQUID signal F is presented in units of uniform current density in the sample as in Fig. 2. The results at $T_c - T < 0.3$ K are also presented on an enlarged $\times 4$ scale. The lower data curve is associated with the left y axis and bottom x axis, the upper curves are associated with the right y axis and top x axis. Note the shift of origin for the right y axis. Different symbols correspond to different warming runs after magnetizing cycles at indicated temperatures. The straight solid lines are the result of linear regression analysis of experimental data taken in the range 0.3 K $< T_c - T <$ 1.1 K. The solid curve is the result of calculations with formulae and fitting parameters presented in the text in Sec. III C.

As can be seen in Fig. 3, the fit is very good. The experimental data are exactly on the straight line in coordinates $(\sqrt{F}, T)$ well below T_c^* showing that locally $j_c \propto (T_c' - T)^2$. Although the experimental data deviate from the straight line as T approaches T_c, the deviations are well described by the same temperature dependence of j_c if one takes into account the inhomogeneity of the critical temperature. All studied samples, prepared by different methods on different substrates, exhibited the same quadratic behavior $j_c \propto (T_c^* - T)^2$ in the range $T_c - T \lesssim 2$ K. The temperature T_c determined as the signal zero point was in the range 87–89 K. The difference between the extrapolated value T_c^* and T_c was $(T_c - T_c^*) < 0.2$ K. The function $F(T)$ varied from sample to sample in the interval around and above T_c^*. We strongly believe that these experimental data prove the quadratic dependence $j_c \propto (T_c - T)^2$ with high precision in spite of the critical temperature inhomogeneity ~ 0.1 K.

In Fig. 3 the solid straight line passing through experimental points in the range 0.3 K $< (T_c - T) <$ 1.1 K, is the result of linear regression analysis of the experimental data in this interval. The deviations from the straight line are less than 0.1%. We checked the accuracy of the power q in the dependence $j_c \propto (T_c - T)^q$ having plotted the experimental data in coordinates $(F^{1/q}, T)$ and repeating the linear regression analysis. The deviations increased with the increasing difference $|q - 2|$. Summarizing the results of this analysis and taking into account the accuracy of critical current and temperature measurements, we can write down the experimentally determined value $q = 2.00 \pm 0.05$. That is the main result of the present work.

To analyze the formation of the time dependent SQUID signal in the presence of sample inhomogeneity is more difficult. We could do it only for smooth and weak variations of the critical current density $\delta j_c(r) \ll \langle j_c \rangle$ and the creep parameter $\delta\sigma(r) \ll \langle \sigma \rangle$. Equation (2) was solved approximately for $\sigma \gg 1$. A solution similar to Eq. (3), but with parameters $j_c = j_c(r)$ and $\sigma = \sigma(r)$ was obtained. From Eq. (1) followed that the time dependence of the SQUID signal approximately retained its form $F(t) \propto (1 + t/t_0)^{-p}$, but the fitting parameters $t_0 = t_0'/\langle \sigma \rangle_1$ and $p = \langle \sigma \rangle_2^{-1}$ might correspond to the differently averaged values $\langle \sigma \rangle_1$ and $\langle \sigma \rangle_2$. The problem of magnetic flux relaxation in the case of strong space variations $\delta j_c(r)$ and $\delta\sigma(r)$ near T_c is much more complicated, and we leave it for the future studies. As curves 2 and 3 in Fig. 1 show, even in this case the magnetic field of circulating superconducting currents at a distance from the film demonstrates a simple power-law time decay. Curve 1 in Fig. 1 is measured so close to T_c that some parts of the sample are already in the normal state. But as the above analysis for $j_c(T)$ showed, the remaining superconducting part is characterized by a very uniform critical temperature, and consequently a uniform creep activation energy. Therefore, without complications due to inhomogeneity one can deduce that the superconducting current decays as $j \propto t^{-1/\sigma}$, even for $\sigma = U_0/kT \simeq 1$.

IV. DISCUSSION

In this section we use the notation for the reduced temperature $\theta \equiv (T_c - T)/T_c$, and introduce the energy scale for vortices

$$\epsilon_0 = \left(\frac{\Phi_0}{4\pi\lambda}\right)^2 = \frac{H_c^2 \xi^2}{2}, \tag{7}$$

which is essentially the superconducting condensation energy within the normal core of radius $\sim\xi$ and unit length, and the GL depairing current[1]

$$j_0 = \frac{4}{3\sqrt{3}} \frac{c\epsilon_0}{\xi\Phi_0} \simeq \frac{c\Phi_0\kappa}{205\lambda^3}. \tag{8}$$

We start with the range $\theta \sim 0.1$ where the mean-field GL theory is valid. The GL penetration depth $\lambda(\theta \simeq 0.1) \simeq 3 \times 10^{-5}$ cm is close to the experimental values measured in Refs. 6,16, and one can estimate $j_0(\theta = 0.1) \simeq 3 \times 10^7$ A/cm^2. The collective pinning theory in the single vortex regime with δT_c pinning in the case of nonoptimal doping[1] gives the values $j_c \simeq j_0 (10^4 \theta)^{-1/3} \sim 0.1 j_0$ at $\theta \sim 0.1$ in agreement with experiment. The theoretical estimates of the pinning barrier U_c in the same temperature range are $U_c \sim kT_c$, significantly lower than the experimental values $U_0 \sim 100kT$. Note that the experimental results on U obtained in the range $\theta \sim 0.1$ in Refs. 10,12 agree with the current data within experimental errors.

There is a simple reason why the theory developed in Ref. 1 either for single-vortex pinning or for pinning of vortex bundles cannot be applied to calculate the creep barriers in thin films. As was shown in Ref. 17, in thin films with $\lambda \gg d$ the interaction of vortices occurs via a magnetic field outside the superconductor. Thus, instead of the interaction $V_{\rm int} \sim e^{-x/\lambda}$, sharply decreasing at a distance $x > \lambda$ due to the screening effect of superconducting currents, one has $V_{\rm int} \sim 1/x$ at $x \gg \lambda_{\rm eff} = \lambda^2/d$. Due to this long-range interaction, all the vortices are involved in the motion of one of them during the flux creep. At the same time the adjustment of the vortex core to the pinning potential which determines the critical current, occurs without disturbing the neighbors because of the very high ratio of λ/ξ. Hence the single vortex pinning theory is valid for j_c but fails for U_c. In the present experiments at $\theta \sim 0.1$, the penetration depth $\lambda \simeq d$, and to some extent the long range vortex interaction is relevant. It becomes even more important when λ grows as $T \to T_c$.

As follows from the mean-field pinning theory,[1] $j_c \propto j_0 \theta^{-1/3} \propto \theta^{7/6}$. The last relation indicates that j_c should decrease approximately linearly with temperature in the relatively narrow interval $10^{-1} \geqslant \theta \geqslant 10^{-3}$. As one can see in Fig. 2, it might be a very crude approximation for $\theta > 0.05$, but it is evidently wrong at $\theta \lesssim 0.01$. The temperature dependence of the creep activation energy U_0 also indicates that in that range the creep mechanism changes. In spite of large scatter of data in Fig. 2 one can see a sharp bend to a steep drop in U_0 at $\theta \simeq 0.01$. At $\theta < 0.01$ the creep barrier is approximately proportional to the reduced temperature, but other exponents $y \approx 1$ in $U_0 \propto \theta^y$, are also possible due to large experimental errors. In the published mean-field theories there is no indication how the creep barrier turns to zero. For bulk samples it is considered constant $\sim kT_c$ up to T_c itself. We suggest that the sharp bend in the curve $U_0(T)$ at $(T_c - T) \sim 1$ K indicates that the region of critical fluctuations has been entered.

A plausible hypothesis about the mechanism of critical fluctuations in the context of flux creep is a generation of vortex-antivortex pairs, which dissociate due to the opposite sign of the Lorentz force in the presence of the current. The antivortex annihilates with a pinned vortex present in the sample. The newly born vortex drifts to a neighboring metastable state in the pinning potential, an elementary step of the flux creep process being thus realized. In this process the creep activation energy is determined not by the pinning potential but by the energy to generate the vortex-antivortex pair. Following Ref. 1 we suppose that the energy to create a vortex-antivortex pair separated by a distance $x > \xi$ and directed perpendicular to the current flow is

$$U(x) = 2\epsilon_0 d \ln\left(\frac{x}{\xi}\right) - \frac{2\Phi_0 j d}{c} x. \tag{9}$$

It should be noted that the logarithmic dependence in the first term is valid for $x \lesssim \lambda$ in the bulk samples, and up to $x \lesssim \lambda_{\rm eff}$ in thin films. The activation energy for the current-assisted thermal unbinding is given by the maximum value of $U(x)$ at the distance $x_m \simeq 2.7\xi(j_c/j)$ as

$$U = 2\epsilon_0 d \ln\left(\frac{j_c}{j}\right),$$

where the critical current density is $j_c = c\epsilon_0/(2.7\xi\Phi_0) \simeq 0.5 j_0$. One can see that the present hypothesis explains the logarithmic dependence of the flux creep activation barrier on the current density, and consequently the observed power-law time decay of the superconducting currents. The GL formulas (7),(8) can be used to extrapolate the low-temperature values to the border of the critical region to obtain theoretical estimates both for $j_0 \simeq 10^6$ A/cm^2 and $U_0 = 2\epsilon_0 d \simeq 140kT$ at $\theta = 0.01$ K. The corresponding experimental values are lower: ~ 10 times for j_c and ~ 3 times for U_0. We suppose that the logarithmic function in Eq. (9) is correct but the factor in front of the logarithm, which was obtained in the mean-field theory, should be modified due to critical fluctuations.

To compare Eq. (9) with experiment in a region still closer to T_c, one needs theoretical estimates in the fluctuation-dominated critical regime. It is well established theoretically that the crossover upon approaching T_c is initially to the intermediate critical regime of a weakly charged superfluid where the fluctuations in ψ are essentially those of an uncharged superfluid or XY model.[9] In this regime, it is shown[3,9] that in three dimensions the coherence length diverges as $\xi \propto \theta^{-2/3}$, the superfluid density scales as $\rho_s \propto \xi^{-1} \propto \theta^{2/3}$, and the penetration depth scales as $\lambda \propto \rho_s^{-1/2} \propto \theta^{-1/3}$. The last result has been confirmed[6] by direct microwave measurements of the penetration depth near T_c down to $\theta \simeq 10^{-3}$. The specific heat measurements[4,5] are consistent with the XY model critical exponent $\alpha \simeq 0$. As has been shown by Lobb,[3] an immediate consequence of this result is that the thermodynamic critical field $H_c \propto \theta$, just as in the GL theory. Both forms of the GL relation in Eq. (7) give the

result for the vortex energy $\epsilon_0 \propto \theta^{2/3}$. It has been argued in Ref. 9 in very general terms that in the intermediate critical regime the characteristic current, which plays the role of the mean-field depairing current, scales as $j_0 \propto \xi^{-2} \propto \theta^{4/3}$. The same result follows from the GL formula in Eq. (8), if one just substitutes the proper scaling for all parameters.

The comparison of $\epsilon_0 \propto \theta^{2/3}$ with the experimental temperature dependence of $U_0(T)$ at $T_c - T < 1$ K is inconclusive due to large experimental errors. But the accurate measurements of the critical current $j_c \propto \theta^2$ definitely disagree with the scaling $j_0 \propto \theta^{4/3}$.

The hypothesis of critical vortex-antivortex generation can be saved by a conjecture that the energy factor in front of the logarithm in Eq. (9) should be modified. This formula follows from the mean-field theory. The second term $\propto j$ is determined by the Lorentz force, and evidently the fluctuations do not change it. But the vortex-antivortex pair interaction could be changed by fluctuations, more and more significantly as $T \to T_c$. To account for this, one tries $\epsilon_0 \to \nu \epsilon_0$ in Eq. (9), introducing a factor $\nu = \nu(\theta)$. Fitting the present data gives $\nu \sim 0.3$ at $\theta = 0.01$. An assumption $\nu \propto \theta^{2/3}$ yields a fairly good agreement for the $U_0 = 2\nu\epsilon_0 d \propto \theta^{4/3}$, and a perfect fit to the critical current scaling $j_c \propto \nu\epsilon_0/\xi \propto \theta^2$. At this stage, in the absence of a flux creep theory in the critical region, we cannot offer any reasons why the vortex-antivortex interaction should be modified as discussed above. Actually, the purpose of our discussion is to stimulate theoretical effort in this area.

V. CONCLUSION

In conclusion, we believe that the critical fluctuations change the flux creep mechanism in the range $(T_c - T) \lesssim 1$ K. This estimate for the critical region width is confirmed by the difference $\Delta T = 0.5$ K between the middle of the resistive transition and the T_c defined as the temperature above which both the critical current and the creep barrier are zero. Considering the ambiguity in the width of the critical region previously discussed in literature, the present results support the traditional Ginsburg criterion $\Delta T = Gi \times T_c \simeq 1$ K.

The power-law time decay of the superconducting currents in the critical region implied that the creep activation energy depended logarithmically on the value j. This result suggested that the critical fluctuations generated vortex-antivortex pairs, but the mean-field energy scale in the vortex pair potential had to be modified to fit the scaling of the 3D XY model to the observed temperature dependence of the critical current $j_c \propto (T_c - T)^2$.

We note that a theory of fluctuation-dominated flux creep is not developed, and many questions about the interpretation of experimental data remain unresolved. Among them is a fundamental question about the applicability of 3D XY scaling in the case of remanent flux creep. The scaling behavior of a weakly charged superfluid was obtained for a zero-field phase transition, whereas the remanent flux creep is intrinsically associated with a finite magnetic field decreasing to zero only at the critical point itself. Further investigations are required to resolve this subtle question.

ACKNOWLEDGMENTS

We are grateful to Torsten Freltoft for a film on a $SrTiO_3$ substrate and helpful discussions, and to Rene Pretorius for support of this work.

[1] G. Blatter, M. V. Feigel'man, V. B. Geshkenbein, A. I. Larkin, and V. M. Vinokur, Rev. Mod. Phys. **66**, 1125 (1994).

[2] Y. Yeshurun, A. P. Malozemoff, and A. Shaulov, Rev. Mod. Phys. **68**, 911 (1996).

[3] C. J. Lobb, Phys. Rev. B **36**, 3930 (1987).

[4] S. E. Inderhees, M. B. Salamon, J. P. Rice, and D. M. Ginsberg, Phys. Rev. B **47**, 1053 (1993); M. B. Salamon, Jing Shi, N. Overend, and M. A. Howson, *ibid.* **47**, 5520 (1993).

[5] N. Overend, M. A. Howson, and I. D. Lawrie, Phys. Rev. Lett. **72**, 3238 (1994).

[6] S. Kamal, D. A. Bonn, N. Goldenfeld, P. J. Hirchfeld, R. Liang, and W. N. Hardy, Phys. Rev. Lett. **73**, 1845 (1994).

[7] S. M. Anlage, J. Mao, J. C. Booth, Dong Ho Wu, and J. L. Peng, Phys. Rev. B **53**, 2792 (1996): J. C. Booth, Dong Ho Wu, S. B. Qadri, E. F. Skelton, M. S. Osofsky, A. Piqué, and S. M. Anlage, Phys. Rev. Lett. **77**, 4438 (1996).

[8] S. J. Hagen, Z. Z. Wang, and N. P. Ong, Phys. Rev. B **38**, 7137 (1988); T. A. Friedmann, J. P. Rice, J. Giapintzakis, and D. M. Ginsberg, *ibid.* **39**, 4258 (1989).

[9] D. S. Fisher, M. P. A. Fisher, and D. A. Huse, Phys. Rev. B **43**, 130 (1991).

[10] M. Konczykowski, A. P. Malozemoff, and F. Holtzberg, Physica C **185-189**, 2203 (1991).

[11] Y. Abulafia, A. Shaulov, Y. Wolfus, R. Prozorov, L. Burlachkov, and Y. Yeshurun, Phys. Rev. Lett. **77**, 1596 (1996).

[12] H. Darhmaoui, J. Jung, J. Talvacchio, M. A-K. Mohamed, and L. Friedrich, Phys. Rev. B **53**, 12 330 (1996).

[13] E. H. Brandt, Phys. Rev. B **50**, 4034 (1994).

[14] J. Zhu, J. Mester, J. Lockhart, and J. Turneaure, Physica C **212**, 216 (1993).

[15] V. M. Vinokur, M. V. Feigel'man, and V. B. Geshkenbein, Phys. Rev. Lett. **67**, 915 (1991).

[16] H. Jiang, T. Yuan, H. How, A. Widom, C. Vittoria, and A. Drehman, J. Appl. Phys. **73**, 5865 (1993).

[17] J. Pearl, Appl. Phys. Lett. **5**, 65 (1964).